Science of the Total Environment 694 (2019) 133740

Contents lists available at ScienceDirect

Science of the Total Environment

journal homepage: www.elsevier.com/locate/scitotenv

Seasonal differences in dissolved organic matter properties and sources in an Arctic fjord: Implications for future conditions

Simona Retelletti Brogi [a], Jin Young Jung [b], Sun-Yong Ha [b], Jin Hur [a,*]

[a] Department of Environment & Energy, Sejong University, Seoul 05006, South Korea
[b] Division of Polar Ocean Science Research, Korea Polar Research Institute (KOPRI), Incheon 21990, South Korea

HIGHLIGHTS

- The seasonal variability of DOM properties in an Arctic fjord was studied.
- DOM features were related to physical chemical and biological fjord characteristics.
- Mycosporine-like amino acids were identified in April but not in October.
- A marked difference in FDOM was observed in the two seasons.
- The FDOM properties in April are driven by melting ice.

GRAPHICAL ABSTRACT

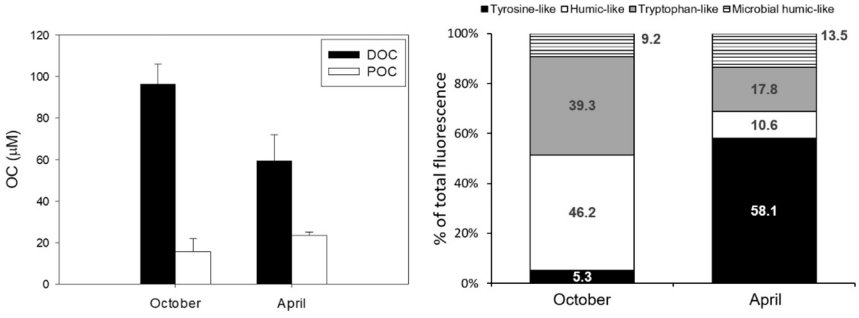

ARTICLE INFO

Article history:
Received 8 May 2019
Received in revised form 31 July 2019
Accepted 1 August 2019
Available online 02 August 2019

Editor: Daniel Wunderlin

Keywords:
Arctic
DOM
EEMs
Chlorophyll-a
Molecular size distribution
Kongsfjorden

ABSTRACT

The Arctic Ocean is undergoing drastic changes due to the effects of climate change. Arctic fjords are preferred systems to study these changes as they respond quickly to variations in ocean, land and atmosphere conditions. In this study, we investigated for the first time the seasonal variability of dissolved organic matter (DOM) properties and its origin in an Arctic fjord, which allows for an assessment of the future potential effects of climate change in this environment. We conducted an integrated analysis of the concentrations, optical properties (absorption and fluorescence), and molecular size distributions of DOM in two seasons (October 2017 and April 2018) and in eight to ten stations in Kongsfjorden (Svalbard) along with the related environmental parameters such as chlorophyll-a, inorganic nutrients, particulate organic carbon (POC), temperature, and salinity. Our results showed that, in both seasons, the DOM in the fjord was predominately of autochthonous origin with a seasonally variable terrestrial input. The dissolved organic carbon (DOC) concentrations were consistently higher in October than in April at each station. Fluorescence spectroscopy revealed a marked seasonal variability depending on the DOM fluorophore types and size fractions. In October, humic-like and tryptophan-like substances were dominant whereas in April, tyrosine-like compounds represented, on average, 58% of the DOM fluorescence. This study points out the key role of spring sea ice melting in determining the DOM properties of the fjord in spring.

1. Introduction

The effects of climate change on the global oceans are already perceptible (Howes et al., 2015; Poloczanska et al., 2016; Saba et al., 2016) with the rapid warming of the Arctic Ocean that causes a drastic

* Corresponding author.
E-mail address: jinhur@sejong.ac.kr (J. Hur).

https://doi.org/10.1016/j.scitotenv.2019.133740
0048-9697/

reduction in multiyear sea ice (IPCC, 2014; Overland and Wang, 2013). These effects are likely to alter the physical and chemical properties of the water masses and, in general, the marine ecosystem. However, they are not yet fully understood (Kortsch et al., 2015; Rosenblatt and Schmitz, 2016; Underwood et al., 2019).

The importance of Arctic fjords is well recognized as they represent the link between the land and the ocean, and they are subjected to intense seasonality with respect to the formation and melting of sea ice, snow, and glaciers. Due to their characteristics, these fjords show a fast response to variations in ocean, land and atmospheric conditions (Cottier et al., 2005; Svendsen et al., 2002). In the Svalbard Archipelago, the influence of Atlantic, Arctic and freshwater inputs on the west coast of Spitsbergen make the fjords in this area very sensitive indicators of such environmental changes (Cottier et al., 2005, 2010).

For these reasons, a number of investigations have been conducted to characterize this area and to examine the changes in a hope to ultimately relate them to climate change. Many previous studies have focused on the oceanographic conditions and water masses (Cottier et al., 2005, 2010; Divya and Krishnan, 2017; Noufal et al., 2017; Svendsen et al., 2002), as well as on phytoplankton (Calleja et al., 2017; Hegseth and Tverberg, 2013). Recently, Iversen and Seuthe (2011) highlighted the importance of the microbial community in the functioning of one of these fjords on west Spitsbergen, Kongsfjorden. The functioning of the microbial food web is strictly related to the quality and concentration of organic matter (Logue et al., 2016; Osterholz et al., 2016). The importance of the links between organic carbon, the microbial food web, and the autotrophic organisms in the Arctic fjord ecosystem has been demonstrated and their variations have been discussed in relation to seasonality and the hydrological conditions (Calleja et al., 2017; Iversen and Seuthe, 2011). Moreover, some studies revealed the close associations of dissolved organic matter (DOM) concentration and properties in Arctic fjords with other biological and environmental parameters such as microbial community, phytoplankton, and inorganic nutrients (Holding et al., 2017; Osterholz et al., 2014; Pavlov et al., 2014). Considering the strong seasonal variability in the fjord with respect to the hydrological and biological conditions, a similar variability in DOM composition and origin can be inferred. Unfortunately, previous studies have focused almost exclusively on either the spring or summer period, and, thus, failed to demonstrate the interseasonal variability. To the best of the authors' knowledge, a rigorous comparison between the properties and the origins of DOM between different seasons in this fjord has not been previously published.

With this background, this study aims to contribute to filling an important knowledge gap by exploring the seasonal variation of DOM properties. The main goals of the study, therefore, are (1) to investigate the concentration, optical and molecular size properties of DOM (i.e., absorption, fluorescence, and molecular size distributions) in spring and autumn (April and October, respectively) in Kongsfjorden (Svalbard); and (2) to relate them to other environmental parameters including hydrological conditions, chlorophyll-a, and nutrients so as to develop a fact-based perspective on the future of this climate-change-sensitive area.

2. Materials and methods

2.1. Studied area

Kongsfjorden is a 27 km long and 4–10 km wide fjord on the northwest coast of Spitsbergen (Fig. 1a). The depth ranges from <100 m in the interior to a maximum of 394 m in the outer parts. Five tidewater glaciers are present in the inner part of the fjord and their seasonal melting affects the fjord between April and July. This fjord receives a low terrestrial input and is alternately dominated by Arctic and Atlantic waters as dictated by the season. A more detailed description of the characteristics of the fjord can be found in Cottier et al. (2010) and the reference therein.

2.2. Sampling

Surface seawater samples were collected from a depth of ~1.0 m in Kongsfjorden (Svalbard Archipelago) in October 2017 and April 2018. Samples were collected from 10 different stations covering the entire fjord (Fig. 1a). Due to the presence of sea ice in the inner extremity of the fjord, stations 3 and 6 were not sampled in April 2018, and the location of stations 2 and 4 were slightly moved with respect to the same stations in October 2017 (white dots in Fig. 1a). Profiles of salinity and temperature were obtained with a CTD (SD204, SAIV A/S, Norway). The samples were collected using a 10-liter Niskin bottle and immediately transferred to the marine laboratory for processing.

2.3. Samples treatment and analytical measurements

Samples for chlorophyll-a (Chl-a) concentration were filtered through 0.7 μm pore size filters (Whatman, GF/F) and the filters were frozen until analysis. Chl-a was extracted in 90% acetone for 24 h at 4 °C (Parson et al., 1984), and quantified using a pre-calibrated Turner Designs model 10-AU fluorometer.

Inorganic nutrients (nitrates, phosphate, silicate) were measured using a four-channel continuous Auto-Analyzer (QuAAtro, Seal Analytical). The precisions for the NO_3^-, PO_4^{3-}, and $Si(OH_4)$ measurements were ± 0.14, ± 0.02, and ± 0.28 μmol L^{-1}, respectively.

For the analysis of particulate organic carbon (POC), the samples were poured from the Niskin bottle into amber polyethylene bottles. Known volumes (500 mL – 1 L) of seawater were filtered onto precombusted Whatman GF/F filters (47 mm) under gentle vacuum (< 0.1 MPa). The filters were stored at −80 °C until the analysis. Before POC analysis, the filters were freeze-dried and exposed to HCl fumes for 24 h in a desiccator to remove inorganic carbon. POC concentrations were measured with a CHN elemental analyzer (vario MACRO cube, Elemental, Germany). Acetanilide was used as a standard. The precision of these measurements was ±4%.

Samples for DOM were filtered through pre-combusted GF/F filters and stored at 4 °C until analysis (within 1 month from the time of collection). Dissolved organic carbon (DOC) and total dissolved nitrogen (TDN) were quantified by using a total organic carbon analyzer (Shimadzu TOC-VCPH) with an analytical reproducibility of <2%. The reliability of the measurements was checked by daily measurement of the DOC Consensus Reference Material (CRM, Hansell, 2005). Dissolved inorganic nitrogen (DIN) was measured by using a Quaatro Autoanalyzer (QuAAtro, Seal Analytical). Dissolved organic nitrogen (DON) was then calculated as the difference between TDN and DIN.

The absorption spectra were recorded between 230 and 700 nm at a 0.5 nm interval using a Shimadzu UV-1800 UV spectrophotometer. The absorption coefficient at 254 nm (a_{254}) was calculated according to the following equation:

$$a_\lambda = (A_\lambda \times 2.303)/l$$

where A_λ represents the absorbance at wavelength λ, and l, the pathlength (0.01 m).

The specific ultraviolet absorption ($SUVA_{254}$) was calculated by dividing the a_{254} by the DOC concentration (Weishaar et al., 2003).

Fluorescence excitation-emission matrices (EEMs) were scanned with a Hitachi F-7000 fluorescence spectrophotometer (Hitachi Inc., Japan) for an excitation wavelength range of 220 and 500 nm (every 5 nm) and an emission wavelength range of 280 and 550 nm (every 1 nm). Post-acquisition data treatment of the EEMs (i.e. blank subtraction and Raman normalization) and Parallel factor analysis (PARAFAC) were carried out in MATLAB (R2017a) using the drEEM toolbox (Murphy et al., 2013). The EEMs were normalized by the integrated Raman band of Milli-Q water according to Lawaetz and Stedmon (2009) so that fluorescence intensities are reported in Raman Units (R.U.). The validation of the PARAFAC model was made by visual

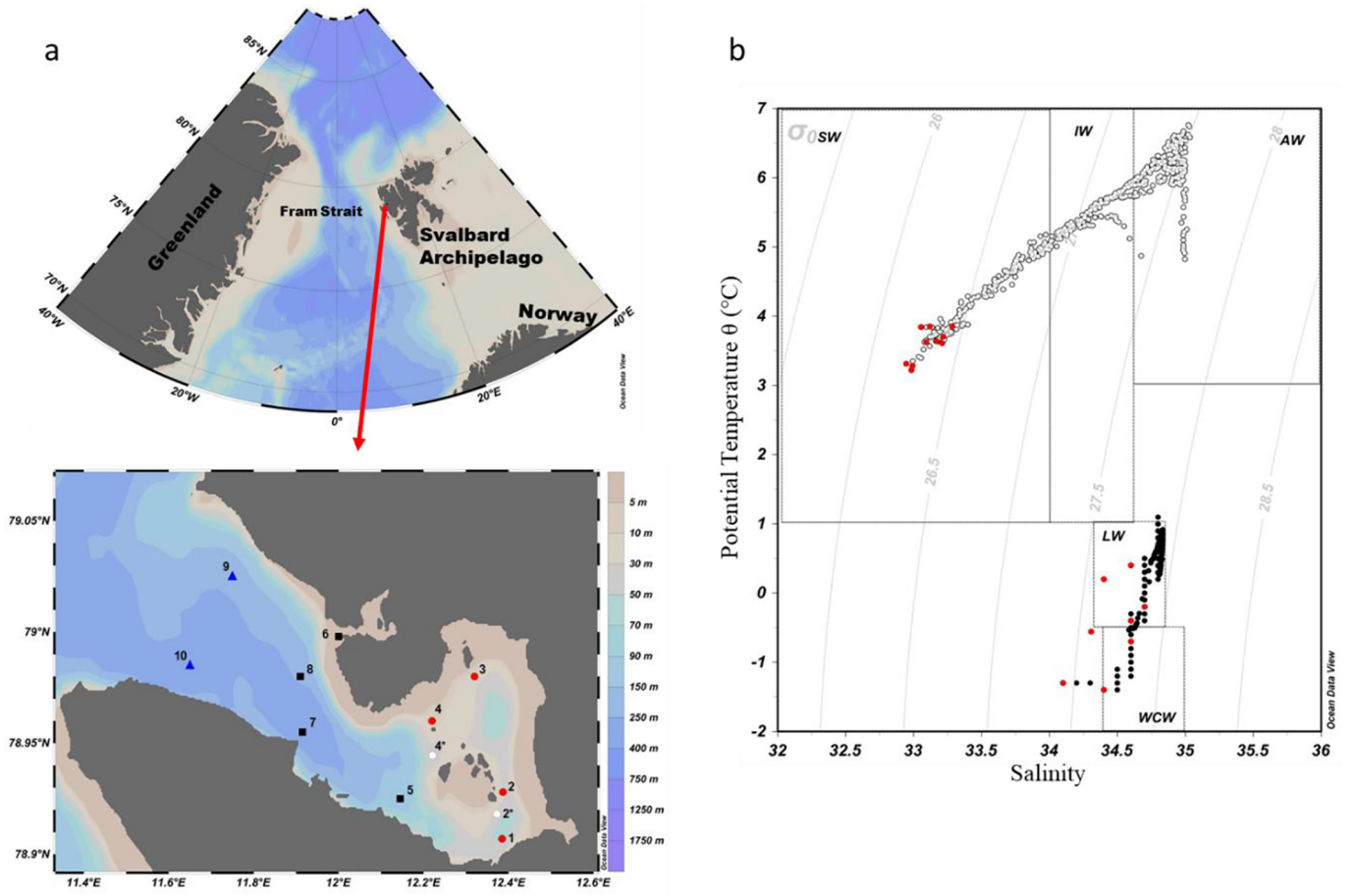

Fig. 1. Study area and water masses identification. (a) Map of the study area and the sampling stations. The circles, squares and triangles represent the inner, central and outer fjord, respectively. (b) θ-S diagram for all the stations. The empty circles designate samples collected in October 2017 and full black circles denote samples collected in April 2018. The red circles represent the surface samples. The dotted frames identify the water masses (Cottier et al., 2005): Surface Water (SW), Intermediate water (IW), Atlantic water (AW), Local Water (LW), and Winter cooled water (WCW). (For interpretation of the references to color in this figure legend, the reader is referred to the web version of this article.)

inspection of the residuals, split half analysis, and percentage of explained variance (98.95%). Specific fluorescence intensity (F_{tot}*) was calculated by dividing the total fluorescence intensity of each sample (sum of the fluorescence of each component) by its DOC concentration. The F_{tot}* provides information on the changes in the composition of the fluorescent DOM as an intrinsic metric (Korak et al., 2014).

DOM molecular size distribution was obtained by a high-performance liquid chromatography system (S-100, Knauer, Berlin, Germany) equipped with an organic carbon detector (OCD) and a size exclusion column (250 mm × 20 mm, TSK, HW 50S, Toso, Japan) (Huber et al., 2011). For each of the two sampling periods, three representative samples (stations 1, 7 and 10) were chosen for the size exclusion chromatography-OCD (SEC-OCD) measurements. The assignments and the quantification of the different size fractions (biopolymers, >10 kDa; humic substances, ~1 kDa; building blocks, 300–500 Da; and low molecular weight, <350 Da) were made using a built-in software and the procedure described in a previous report (Huber et al., 2011) (Fig. S1).

2.4. Statistics

To test the significance of the differences between the two seasons and between different areas within the fjord (inner, central and outer fjord), the Kruskal-Wallis test was performed using the R software. Differences were considered significant for $p \leq 0.05$.

3. Results

In the present study, the 10 stations sampled (8 in April) have been divided into three areas: the outer fjord (stations 9 and 10), the central fjord (stations 5 to 8), and the inner fjord (stations 1 to 4). It is notable that, despite its physical location inside the fjord, the characteristics of station 5 (i.e., bottom depth and θ-S properties) were similar to the stations categorized as the central fjord.

3.1. Temperature and salinity

The potential temperature (θ) in the fjord ranged between ~3 and 7 °C in October and between ~1 and −1.5 °C in April (Fig. 1b). The salinity ranged between 33 and 35 in October, whereas a narrower range, 34.1–34.8, was observed in April (Fig. 1b). According to their θ-S properties and following the classification proposed by Cottier et al. (2005), five different water masses were identified (dashed boxes in Fig. 1b). In October, the Surface Water (SW, $T > 1$ °C, $S < 34$) occupies the first 25–50 m of the water column, while the Intermediate Water (IW, $T > 1$ °C, $34.00 < S < 34.65$) was found between 25 and 50 and 75 m depth. The water column below 75 m is characterized by the presence of the warmer and more saline Atlantic Water (AW, $T > 3$ °C, $S > 34.65$). In April, two water masses were dominant. The Winter Cooled Water (WCW, $T < -0.5$ °C, $34.4 < S < 35.0$) occupies the entire water column in the shallow inner part of the fjord where the maximum depth is <60 m (Stations 1, 2 and 4) and the first ~10 m at station 10. In the rest of

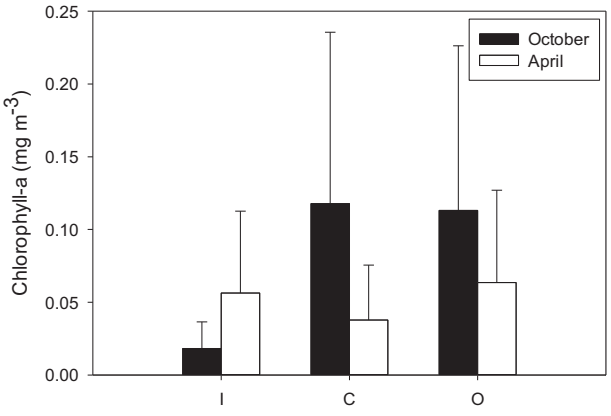

Fig. 2. Average concentrations of chlorophyll-a in the inner (I), central (C), and outer (O) regions of the fjord in the two seasons. Error bars represent the standard deviations of the stations in each area.

the fjord, the majority of the water column is characterized by the presence of the Local Water (LW, $-0.5 < T < 1.0$ °C, $34.30 < S < 34.85$).

3.2. Chlorophyll-a and inorganic nutrients

The concentration of chlorophyll-a ranged between 0.01 and 0.15 mg m^{-3} in October and between 0.03 and 0.09 mg m^{-3} in April (Fig. 2). This difference was, however, not significant ($p = 0.72$). In October, the concentration in the inner fjord is, on average, 4 times lower than those of the central and outer fjord, whereas in April, the difference between the three regions was not significant.

The concentrations of inorganic nutrients were higher in April than in October ($p = 0.0004$, Fig. 3). Total nitrate ($NO_2^- + NO_3^-$) ranged between 0.57 and 3.57 μM in October (average 1.78 ± 0.82 μM), and between 7.07 and 7.92 μM in April (average 7.41 ± 0.29 μM). $Si(OH)_4$ ranged between 1.53 and 2.00 μM in October (average 1.76 ± 0.18 μM), and between 4.35 and 4.85 μM in April (average 4.56 ± 0.15 μM). PO_4^{3-} ranged between 0.06 and 0.16 μM in October (average 0.12 ± 0.03 μM), and between 0.60 and 0.64 μM in April (average 0.63 ± 0.01 μM). No significant differences were found between the inner, central and outer fjord for each season ($p > 0.05$).

3.3. Organic matter concentrations and properties

The concentrations of both DOC and DON were significantly higher in October than in April ($p = 0.0004$ for DOC, $p = 0.0008$ for DON, Fig. 4). DOC ranged between 82 and 112 μM in October (average 96.4 ± 9.5 μM), and between 37 and 77 μM in April (average 59.4 ± 12.7 μM). Spatially, higher DOC values were observed in the central fjord in October ($p = 0.03$), whereas in April there were no significant differences between the three categorized regions. DON ranged between 8 and 13 μM in October (average 10.1 ± 1.3 μM), and between 2 and 9 μM in April (average 5.7 ± 2.5 μM). Unlike the spatial variation of DOC (in April), differences in DON were not observed between the three regions in both seasons. The carbon to nitrogen ratio (C:N) was calculated as the ratio of DOC to DON. The DOC:DON values were highly variable in both seasons, changing between 6 and 13 in October and between 6 and 30 in April (Table S1) but the seasonal or regional differences were not significant. However, it is worth noting that the highest values were observed at stations 1 and 2 in April (i.e., 30 and 15, respectively, Table S1).

The POC seasonal and regional trends were different from those of DOC. In October, it ranged between 11 and 30 μM (average 15.7 ± 6.1 μM), showing significantly higher concentrations in the inner fjord. The POC concentrations in April were higher ($p = 0.004$), ranging between 21 and 25 μM (average 23.6 ± 1.5 μM), but no regional differences were observed.

The DOM absorbance spectra showed different features between the two seasons (Fig. 5). In October, the spectra showed a featureless exponential decrease at increasing wavelengths, typical of open sea DOM. In April, on the other hand, two shoulders, at 270 nm and at 330 nm, were observed in some of the samples (Fig. 5). Neither between the two seasons nor between the three regions of the fjord were the values of the absorption at 254 nm (a_{254}) statistically different although the highest a_{254} values were observed in April at stations 1, 4, and 10 (Table S1). $SUVA_{254}$ values were significantly higher in April (7.05 ± 4.47) than in October (1.96 ± 0.32). The differences between the three regions were not significant. However, the highest $SUVA_{254}$ values were observed in April at stations 1, 4, and 10 (Table S1).

The elaboration of the fluorescence EEMs with PARAFAC validated a 4-component model (Fig. S3). The identification of the components and the attribution of their characteristics to specific fluorophore groups were performed by (i) matching them with the spectra in the Open Fluor database (Murphy et al., 2014), and (ii) comparing the excitation and emission maxima with published components not present in the database (Table S3). Component 1 ($C1_{tyr}$; Ex/Em, 270/304) and component 3 ($C3_{trp}$; Ex/Em 275/338) showed the spectral characteristics typical of protein-like substances. In particular, C1 was attributed to tyrosine-like compounds (Chen et al., 2018; Coble, 2007; D'Andrilli et al., 2019; Kowalczuk et al., 2013; Woods et al., 2011), whereas C3 was interpreted as tryptophan-like compounds (Asmala et al., 2018; Cawley et al., 2012; D'Andrilli et al., 2019; Jørgensen et al., 2011; Nimptsch et al., 2015). Component 2 ($C2_h$; Ex/Em, <250,320/455) and component 4 ($C4_{mh}$; Ex/Em 295/405) showed the typical spectral features of humic-like substances. Compared to $C4_{mh}$, $C2_h$ had the excitation and emission maxima at longer wavelengths. These characteristics have usually been explained by the presence of recalcitrant, terrestrial humic-like materials (Chen et al., 2017; D'Andrilli et al., 2019; Derrien et al., 2018; Retelletti Brogi et al., 2018; Wünsch et al., 2018a; Yang et al., 2019). The spectral characteristics of $C4_{mh}$ with the maxima at lower wavelengths have been attributed to the so-called microbial humic-like compounds. These compounds have been defined as a type of humic-like substances that have been re-elaborated in situ by the microbial community (Lapierre and Del

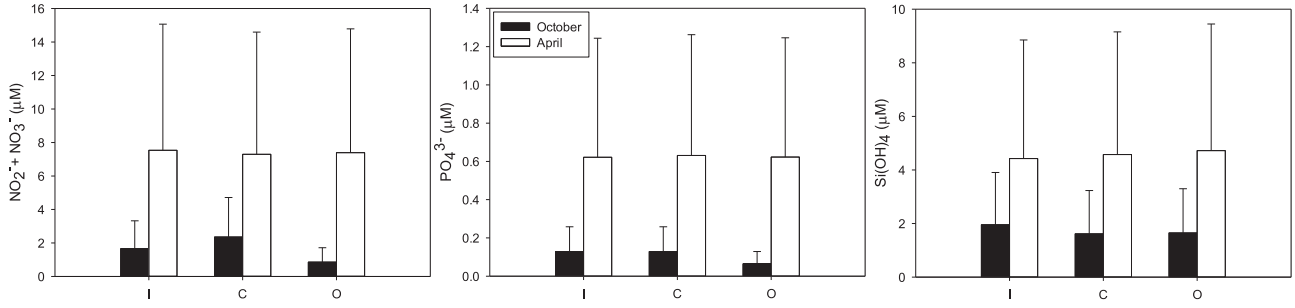

Fig. 3. Average concentrations of nitrate, phosphate, and silicate in the inner (I), central (C), and outer (O) regions of the fjord in the two seasons. Error bars represent the standard deviations of the stations in each area.

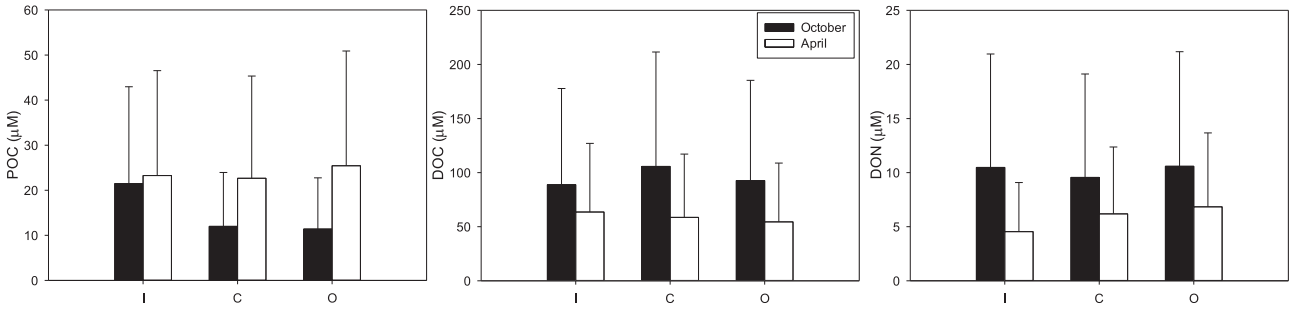

Fig. 4. Average concentrations of particulate organic carbon (POC), dissolved organic carbon (DOC) and nitrogen (DON) in the inner (I), central (C), and outer (O) regions of the fjord in the two seasons. Error bars represent the standard deviations of the stations in each area.

Giorgio, 2014; Søndergaard et al., 2003; Woods et al., 2011; Wünsch et al., 2018b; Yang et al., 2019).

The DOM fluorescence showed a substantial difference between the two seasons. In April, the total fluorescence was on average ~15 times higher than in October (average total fluorescence: 0.12 ± 0.05 R.U. in October and 1.18 ± 1.92 R.U. in April) although no regional differences were observed in both seasons. Similar to $SUVA_{254}$, the highest values were observed in April at stations 1, 4 and 10 (Table S1). Besides the difference in the intensity of the fluorescence between the two seasons, a marked discrepancy was also observed in the relative contribution of the components (Fig. 6). In October, a large fraction of the fluorescence is represented by the terrestrial humic-like compounds ($C2_h$, 46.2 ± 9.8%), followed by the tryptophan-like ($C3_{trp}$, 39.3 ± 11.6%), the microbial humic-like ($C4_{mh}$, 9.2 ± 1.5%), and the tyrosine-like ($C1_{tyr}$, 5.3 ± 5.7%) components. In contrast, in April, the tyrosine-like components ($C1_{tyr}$) represented ~ 58 ± 20% of the total fluorescence, followed by the tryptophan-like ($C3_{trp}$, 17.8 ± 8.2%), the microbial humic-like ($C4_{mh}$, 13.5 ± 6.0%), and the terrestrial humic-like ($C2_h$, 10.6 ± 9.8%) components. In general, the results found in April relative to those in October can be summarized as a significant increase in $C1_{tyr}$, a significant decrease in $C2_h$ and $C3_{trp}$, and a minor variation in $C4_{mh}$.

In April, a good correlation was found between a_{270} (or a_{330}) and $C1_{tyr}$ ($R^2 = 0.98$, $p = 0.0001$ for a_{270}; $R^2 = 0.92$, $p = 0.0001$ for a_{330}, Fig. S4). The correlations of the two absorption coefficients (i.e., a_{270} and a_{330}) with $C3_{trp}$ ($R^2 = 0.90$, $p = 0.0003$ for a_{270}; $R^2 = 0.63$, $p = 0.002$ for a_{330}) were less strong than those with $C1_{tyr}$ (Fig. S4). There were no significant correlations with the other fluorescent components or any other measured parameters. Such good relationships between the absorption coefficients and the protein-like components were not observed for the samples collected in October.

Due to the large variability of the DOC concentrations among the samples (or seasons), the molecular size fractions identified by the SEC-OCD are presented as percentages of total DOC (Table S1). Among the identified size fractions, the biopolymer (BP) fraction, the largest size fraction, was the least abundant, representing only 3–4% and 1–2% of DOC in October and April, respectively (Fig. 7). The size fraction of humic substances (HS) was more abundant in October, ranging between 23 and 33% (average 29%) of total DOC relative to 16 to 25% (average 20%) in April (Fig. 7), which agreed well with the previous result of total DOM fluorescence. The so-called building blocks (BB) represent small sized humic substances and are, thus, thought to be the byproduct from the breakdown of HS. These compounds represented 9–15% (average 12%) and 5–13% (average 8%) of total DOC in October and April, respectively. The low molecular weight (LMW) fraction was the most abundant in both seasons. In April, however, the LMW showed a higher percentage of DOC (60–71%, average 66%) compared to October (49–65%, average 55%). This fraction contains small sized compounds derived from the degradation of the larger molecules and may indicate the strong activity of the microbial community in breaking down high molecular weight compounds into smaller compounds (Penru et al., 2013; Retelletti Brogi et al., 2018).

4. Discussion

4.1. Spring versus autumn: contrasting fjord characteristics

The θ-S properties of the fjord waters clearly indicate the control of different hydrological conditions between the two seasons, in agreement with previous studies (Cottier et al., 2005, 2010; Noufal et al., 2017; Svendsen et al., 2002). In October, a good stratification of the

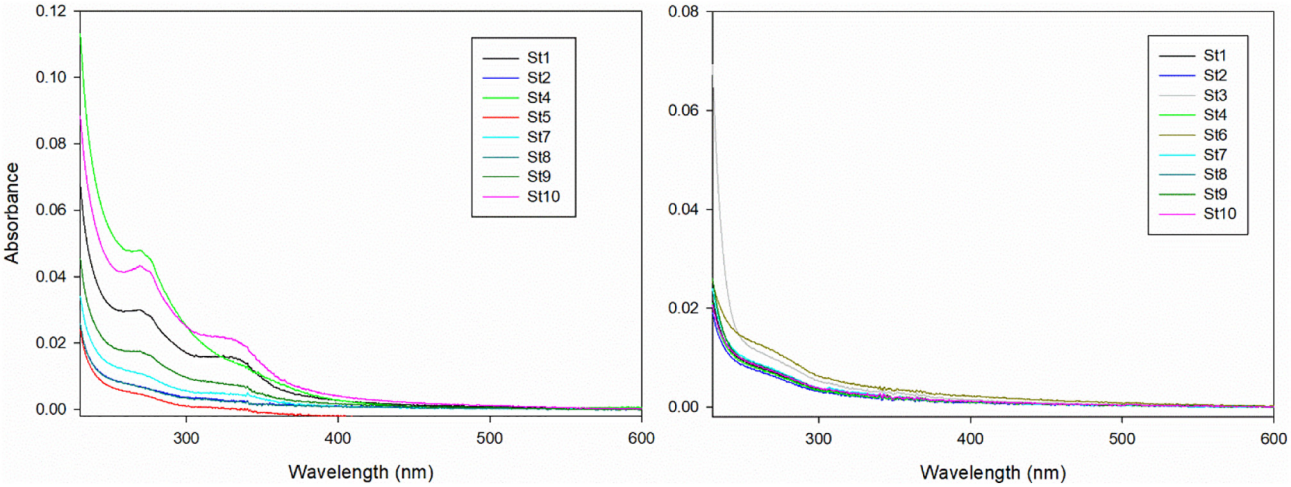

Fig. 5. Absorbance spectra of DOM samples in April (left) and October (right).

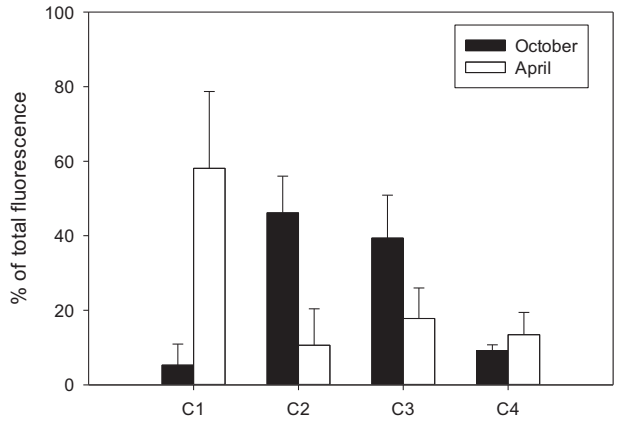

Fig. 6. Average contribution to total fluorescence of the four components in the two seasons. Error bars represent the standard deviations of the stations in each period.

water masses was observed throughout all the fjord sites (Fig. S2 a and b), with the colder and less saline SW in the surface and the denser IW and AW underneath. In April, in stark contrast, a well-mixed water column was observed (Fig. S2 c and d). However, the temperature and salinity were different between the inner fjord and the central/outer fjord. The inner fjord water column and a small thin layer on the surface at station 10 were characterized by colder and less saline WCW, whereas in the rest of the fjord, the temperature and salinity were higher (Fig. S2 c and d). This spatial difference in April can be attributed to the partial melting of the sea ice and glaciers due to spring warming that contributes fresher and colder waters. The inner part of the fjord is characterized by the presence of five tidewater glaciers and, in April 2018, the inner extremity of the fjord and some coastal regions (i.e. close to station 10) were still occupied by sea ice.

The very low concentration of chlorophyll-a in both periods implies a low primary production. In good agreement with the low chlorophyll-a, the inorganic nutrients in April were observed in high concentrations, suggesting a pre-bloom condition in which nutrients are yet to be utilized. This high concentration of nutrients in April can be attributed to the remineralization processes occurring during winter mediated by the heterotrophic microbial community (Iversen and Seuthe, 2011), to the supply of nutrients from melting glaciers (Calleja et al., 2017), and to the mixing of the water column that allows the input of nutrients from deeper waters. Meanwhile, the lower concentrations of nutrients in October imply a condition in which the nutrients consumed during the previous bloom have not been replaced yet. Moreover, the stratification of the water column prevents the supply of nutrients from deeper waters. The concentrations of chlorophyll-a and nutrients were

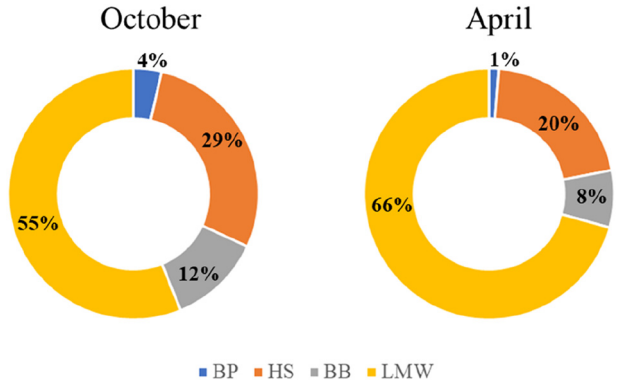

Fig. 7. Relative proportions of the four different size fractions of DOM in the two seasons (average of the three samples measured for each season is presented). BP = Biopolymers (MW > 10 kDa), HS = Humic Substances (MW ~ 1 kDa), BB = Building Blocks (MW 300–500 Da), LMW = Low molecular weight (MW < 350 Da).

consistent with the results reported by Iversen and Seuthe (2011) in Kongsfjorden in pre-bloom condition and in autumn (March and September, respectively, in their study).

Such seasonal differences were also reflected in the concentration of POC. The higher POC observed in April can be explained by the input of melting glaciers. These results are in good agreement with the study published by D'Angelo et al. (2018) that reported the fluxes and the composition of particles in Kongsfjorden over a period of 6 years. The authors observed a higher abundance of POC in spring versus winter. Moreover, in spring, most of the POC was found to originate from newly produced phytoplankton cells, whereas during the winter months, POC was mainly constituted by terrestrial OM.

4.2. Seasonal variation of DOM concentration and properties

The marked seasonal differences were well reflected in DOM concentration and composition. Briefly, in October, higher concentrations of DOC and DON, but lower presence of UV-absorbing (or CDOM) and fluorescent DOM were observed. The DOM fluorescence was dominated by the humic-like ($C2_h$) and tryptophan-like ($C3_{trp}$) components in the season. In April, however, a lower DOC concentration was observed in correspondence with the predominance of the tyrosine-like component ($C1_{tyr}$). Moreover, the absorption spectra of some samples in April exhibited distinctive peaks at 270 and 330 nm.

The higher concentrations of LMW and autochthonous FDOM components ($C1_{tyr} + C3_{trp} + C4_{mh}$) and the low DOC:DON ratios in both seasons indicate the prevalence of the compounds produced in situ rather than terrestrial materials. This is consistent with the very low terrestrial input in this area compared to the rest of the Eurasian Basin where the terrestrial DOM is dominant (Anderson and Amon, 2015; Gonçalves-Araujo et al., 2016; Stedmon et al., 2011a). The higher DOC concentration in October can be attributed to an accumulation of the DOC released/produced during the spring and summer by phytoplankton and microbial community. Regarding these observations, it is worthy to note that a previous study by Iversen and Seuthe (2011) reported similar results. These authors suggested that the DOC that accumulated during spring and summer might serve as a carbon reserve for the microbial community in winter.

On the other hand, the lower DOC in April suggests that the winter reserves have been consumed and that the microbial community has mineralized a part of this DOM into inorganic nutrients, which would reach their maximum concentrations before the spring phytoplankton bloom. The CDOM absorption shoulder at 330 nm reflects the presence of mycosporine-like amino acids (MAAs) (Vernet and Whitehead, 1996). Whereas the peak at 270 nm has been attributed to the presence of MAAs precursor and nucleic acids (Granskog et al., 2015) and in general has been related to the presence of algal DOM (Granskog et al., 2015; Müller et al., 2013; Wozniak and Dera, 2007). MAAs are water-soluble compounds with a MW <400 Da, which are produced by phytoplankton, bacteria, cyanobacteria, and algae in stress conditions, in particular, as sunscreen protection (Cockell and Knowland, 1999; Oren and Gunde-Cimerman, 2007; Řezanka et al., 2004). It is not surprising that these compounds are likely to be produced in this period of the year (i.e., April) with approximately 20 h of sunlight per day (versus 5 h per day in October). The presence of these compounds in Kongsfjorden was previously reported and their variability has been related to the phytoplankton composition (Ha et al., 2012). In stations where these peaks were more evident, the fluorescence of $C1_{tyr}$ and $C3_{trp}$ were exceptionally higher (i.e., station 1, 4 and 10). The good correlations found in April between the absorption coefficients (i.e. a_{270} and a_{330}) and the protein-like components ($C1_{tyr}$ and $C3_{trp}$) suggest that the MAAs (a_{330}) and algal DOM (a_{270}) significantly contributed to the DOM tyrosine-like fluorescence, and therefore to most of the DOM fluorescence in April. It is noteworthy that these signals were more evident for the stations close to the melting sea ice, a good correlation was indeed found between a_{330} and salinity (Spearman rank correlation, p

= 0.042, Rho = −0.75). The close intercorrelations between the highest values of $C1_{tyr}$ and $C3_{trp}$, the MAAs/algal DOM absorbance signals, and the melting ice suggest that most of these compounds might derive directly or indirectly from the melting ice itself. Several studies have reported the presence of MAAs in the sea ice and their significant contribution to UV absorption (Arrigo and Thomas, 2004; Fritsen et al., 2011; Granskog et al., 2015; Norman et al., 2011; Uusikivi et al., 2010). Moreover, an accumulation of protein-like compounds within the ice has been observed and attributed to the activity of the algal and microbial ice community (Granskog et al., 2015; Müller et al., 2011; Retelletti Brogi et al., 2018; Stedmon et al., 2011b). Granskog et al. (2015) suggested that although the sea ice melting may not be the supplier of CDOM, it can be responsible for the production of specific types of CDOM, which include some light-absorbing compounds produced within the ice (e.g. MAAs). Such an explanation is consistent with the pronounced differences in fluorescent components and in the shape of absorption spectra between the two seasons (i.e. the presence of two shoulders at 270 nm and 330 nm in April) in the present study. Meanwhile, the higher F_{tot}^* values (i.e. total fluorescence normalized by DOC, Table S1) in April versus October indicate that the DOM molecules found in April are intrinsically more fluorescent.

The marked seasonal dissimilarity in the fluorescence of $C2_h$ and $C3_{trp}$ may be the result of the complex operation of several factors. First, the higher $C2_h$ fluorescence in October, in agreement with a higher abundance of the HS and BB fractions, may be explained by a hypothesis regarding the contribution of POC degradation. The decoupling in the concentration between POC and DOC (i.e., low POC but high DOC) in October suggests that POC degradation may partially contribute to the higher DOC. Since in this period most of the POC is attributed to terrestrial OM (D'Angelo et al., 2018), it is reasonable to infer that the POC degradation, which releases DOC would increase the content of humic substances rather than fresh materials. Moreover, humic substances are known to be easily photodegraded (Cory et al., 2007; Liu et al., 2010; Osburn et al., 2009), and, therefore, their fluorescence is likely to be lower in April under high irradiation. The higher irradiation can also partially explain the reduction of $C3_{trp}$ in April. Mayer et al. (1999) have shown that tryptophan-like compounds are more sensitive to photodegradation than tyrosine-like compounds. Secondly, the strong linear relationship between $C3_{trp}$ and a_{270} implies that this component is partially affected by ice melting. Previous studies revealed the fundamental role of the microbial community, fueled by DOM, in the functioning of the Kongsfjorden ecosystem in all seasons (Iversen and Seuthe, 2011). Due to the strong interconnection between the microbial community and DOM, it can be assumed that the variations in abundance and activity of the microbes in different seasons may also affect the changes of the DOM properties. The lower activity of the microbial food web reported by Iversen and Seuthe (2011) in autumn (September in their case) can be explained by the higher percentage of humic-like compounds. On the other hand, a higher bacterial production observed in spring by Iversen and Seuthe (2011) might be attributed to an increase of labile compounds from sea ice melting.

4.3. Implications for expected future changes in DOM inputs

Multi-year monitoring of oceanographic conditions (2–3 years) showed a progressive warming of the fjord and an increasing Atlantic Water intrusion (Divya and Krishnan, 2017; Noufal et al., 2017; Tverberg et al., 2019). This warming is expected to result in: 1) an acceleration of seasonal sea ice melting (Divya and Krishnan, 2017); 2) an increased melting rate and retreat of the glaciers (Hanna et al., 2009; Luckman et al., 2015); and 3) an enhancement of the stratification of the water column. The increase in glacier melting and an increase in winter precipitation (Førland et al., 2011) are likely to bring more sediments, and, therefore, POC from the land (D'Angelo et al., 2018). Both the increased particle fluxes, which reduce photosynthetic active radiation (PAR) penetration, and the enhanced stratification preventing the upwelling of nutrients will affect (i.e. reduce) primary production.

By reflecting the results from the present study against the backdrop of the anticipated effects of climate change as mentioned above, some hypotheses can be suggested. First, it is possible that the increased glacier melting and POC fluxes will increase the humic-like materials in the fjord. Second, a reduced primary production likely leads to a decrease in autochthonous DOM during and after spring phytoplankton bloom. Moreover, two different future scenarios can be presented concerning the possible effect of ice melting on DOM. Some studies anticipated the increase in autochthonous and bioavailable DOM due to an increase in sea ice melting (Underwood et al., 2019), which agrees with our results that highlighted the importance of sea ice DOM in producing protein-like compounds. However, other recent studies reported a decrease in the formation of seasonal sea ice in this area (Arntsen et al., 2019; Isaksen et al., 2016). This reduction may, on a longer time scale, drastically limit the input/production of these labile compounds. Due to the strong dependence of the microbial community on the amount and quality of DOM (Logue et al., 2016; Osterholz et al., 2016), these expected variations in DOM properties with the progress of warming might ultimately have critical effects on the microbial loop, which will in turn most likely affect the upper trophic levels.

5. Conclusions

The results of this study confirmed previous findings that the fjord is dominated by autochthonous materials and receives very low terrestrial inputs. Marked differences in DOM optical properties were observed between the two periods, which was greater than and opposite to the variation in DOC. Through the analysis of the absorption spectra of CDOM, it was possible to identify the presence of unique compounds produced in situ as sunscreen (i.e. mycosporine-like amino acids). These results highlighted the key role of spring sea ice melting, and to a minor extent, glacier melting, in shaping the DOM optical properties of the fjord, and, presumably, DOM bioavailability. The close link between DOM and ice melting suggest that Arctic DOM dynamics and composition could be highly affected by future climate change, which is predicted to drastically reduce the sea ice formation/cover in the future.

In this context, more research effort should be invested to predict the effect of a reduced pulse of organic matter driven by the decline in the sea ice through in situ experiments and models based on an extensive spatial and temporal sampling scheme to characterize DOM in these Arctic fjords.

Acknowledgements

This work was supported by a National Research Foundation of Korea (NRF) grant funded by the Korean government (MSIP) (No. 2017R1A4A1015393) and also by the Korea Polar Research Institute Grants PM18050 (KIMST Grant 20160247) and PE19170. We are especially grateful to Dr. Ikechukwu A. Ike for his careful English proofreading.

Appendix A. Supplementary data

Supplementary data to this article can be found online at https://doi.org/10.1016/j.scitotenv.2019.133740.

References

Anderson, L.G., Amon, R.M.W., 2015. DOM in the Arctic ocean. Biogeochemistry of Marine Dissolved Organic Matter, Second edition, pp. 609–633 https://doi.org/10.1016/B978-0-12-405940-5.00014-5.

Arntsen, M., Sundfjord, A., Skogseth, R., Błaszczyk, M., Promińska, A., 2019. Inflow of warm water to the inner Hornsund fjord, Svalbard; exchange mechanisms and influence on local sea ice cover and glacier front melting. J. Geophys. Res. Ocean. https://doi.org/10.1029/2018JC014315.

Arrigo, K.R., Thomas, D.N., 2004. Large scale importance of sea ice biology in the Southern Ocean. Antarct. Sci. 16, 471–486. https://doi.org/10.1017/S0954102004002263.
Asmala, E., Haraguchi, L., Markager, S., Massicotte, P., Riemann, B., Staehr, P.A., Carstensen, J., 2018. Eutrophication leads to accumulation of recalcitrant autochthonous organic matter in coastal environment. Glob. Biogeochem. Cycles 32, 1673–1687. https://doi.org/10.1029/2017GB005848.
Calleja, M.L., Kerhervé, P., Bourgeois, S., Kędra, M., Leynaert, A., Devred, E., Babin, M., Morata, N., 2017. Effects of increase glacier discharge on phytoplankton bloom dynamics and pelagic geochemistry in a high Arctic fjord. Prog. Oceanogr. 159, 195–210. https://doi.org/10.1016/j.pocean.2017.07.005.
Cawley, K.M., Butler, K.D., Aiken, G.R., Larsen, L.G., Huntington, T.G., McKnight, D.M., 2012. Identifying fluorescent pulp mill effluent in the Gulf of Maine and its watershed. Mar. Pollut. Bull. 64, 1678–1687. https://doi.org/10.1016/J.MARPOLBUL.2012.05.040.
Chen, M., Kim, S.-H.H., Jung, H.-J.J., Hyun, J.-H.H., Choi, J.H., Lee, H.-J.J., Huh, I.-A.A., Hur, J., 2017. Dynamics of dissolved organic matter in riverine sediments affected by weir impoundments: production, benthic flux, and environmental implications. Water Res. 121, 150–161. https://doi.org/10.1016/J.WATRES.2017.05.022.
Chen, M., Jung, J., Lee, Y.K., Hur, J., 2018. Surface accumulation of low molecular weight dissolved organic matter in surface waters and horizontal off-shelf spreading of nutrients and humic-like fluorescence in the Chukchi Sea of the Arctic Ocean. Sci. Total Environ. 639, 624–632. https://doi.org/10.1016/J.SCITOTENV.2018.05.205.
Coble, P.G., 2007. Marine optical biogeochemistry: the chemistry of ocean color. Chem. Rev. 107, 402–418. https://doi.org/10.1021/cr050350+.
Cockell, C.S., Knowland, J., 1999. Ultraviolet radiation screening compounds. Biol. Rev. 47, 311–345. https://doi.org/10.1111/j.1469-185X.1999.tb00189.x.
Cory, R.M., McKnight, D.M., Chin, Y.P., Miller, P., Jaros, C.L., 2007. Chemical characteristics of fulvic acids from Arctic surface waters: microbial contributions and photochemical transformations. J. Geophys. Res. Biogeosci. 112, G4. https://doi.org/10.1029/2006JG000343.
Cottier, F., Tverberg, V., Inall, M., Svendsen, H., Nilsen, F., Griffiths, C., 2005. Water mass modification in an Arctic fjord through cross-shelf exchange: the seasonal hydrography of Kongsfjorden, Svalbard. J. Geophys. Res. Ocean. 110, C12005. https://doi.org/10.1029/2004JC002757.
Cottier, F.R., Nilsen, F., Skogseth, R., Tverberg, V., Skarðhamar, J., Svendsen, H., 2010. Arctic fjords: a review of the oceanographic environment and dominant physical processes. Geol. Soc. London, Spec. Publ. 344, 35–50. https://doi.org/10.1144/SP344.4.
D'Andrilli, J., Junker, J.R., Smith, H.J., Scholl, E.A., Foreman, C.M., 2019. DOM composition alters ecosystem function during microbial processing of isolated sources. Biogeochemistry 142, 281–298. https://doi.org/10.1007/s10533-018-00534-5.
D'Angelo, A., Giglio, F., Miserocchi, S., Sanchez-Vidal, A., Aliani, S., Tesi, T., Viola, A., Mazzola, M., Langone, L., 2018. Multi-year particle fluxes in Kongsfjorden, Svalbard. Biogeosciences 15, 5343–5363. https://doi.org/10.5194/bg-15-5343-2018.
Derrien, M.M., Kim, M.-S.M., Ock, G.G., Hong, S.S., Cho, J.J., Shin, K.-H.K.-H., Hur, J., 2018. Estimation of different source contributions to sediment organic matter in an agricultural-forested watershed using end member mixing analyses based on stable isotope ratios and fluorescence spectroscopy. 618, 569–578.
Divya, D.T., Krishnan, K.P., 2017. Recent variability in the Atlantic water intrusion and water masses in Kongsfjorden, an Arctic fjord. Polar Sci 11, 30–41. https://doi.org/10.1016/j.polar.2016.11.004.
Førland, E.J., Benestad, R., Hanssen-Bauer, I., Haugen, J.E., Skaugen, T.E., 2011. Temperature and precipitation development at Svalbard 1900–2100. Adv. Meteorol. https://doi.org/10.1155/2011/893790.
Fritsen, C.H., Wirthlin, E.D., Momberg, D.K., Lewis, M.J., Ackley, S.F., 2011. Bio-optical properties of Antarctic pack ice in the early austral spring. Deep. Res. Part II Top. Stud. Oceanogr. 58, 1052–1061. https://doi.org/10.1016/j.dsr2.2010.10.028.
Gonçalves-Araujo, R., Granskog, M.A., Bracher, A., Azetsu-Scott, K., Dodd, P.A., Stedmon, C.A., 2016. Using fluorescent dissolved organic matter to trace and distinguish the origin of Arctic surface waters. Sci. Rep. 6, 33978. https://doi.org/10.1038/srep33978.
Granskog, M.A., Nomura, D., Müller, S., Krell, A., Toyota, T., Hattorl, H., 2015. Evidence for significant protein-like dissolved organic matter accumulation in Sea of Okhotsk sea ice. Ann. Glaciol. 56, 1–8. https://doi.org/10.3189/2015AoG69A002.
Ha, S.Y., Kim, Y.N., Park, M.O., Kang, S.H., Kim, H.C., Shin, K.H., 2012. Production of mycosporine-like amino acids of in situ phytoplankton community in Kongsfjorden, Svalbard, Arctic. J. Photochem. Photobiol. B Biol. 114, 1–14. https://doi.org/10.1016/j.jphotobiol.2012.03.011.
Hanna, E., Cappelen, J., Fettweis, X., Huybrechts, P., Luckman, A., Ribergaard, M.H., 2009. Hydrologic response of the Greenland ice sheet: the role of oceanographic warming. Hydrol. Process. 23, 7–30. https://doi.org/10.1002/hyp.7090.
Hansell, D.A., 2005. Dissolved organic carbon reference material program. EOS Trans. Am. Geophys. Union 86, 318. https://doi.org/10.1029/2005EO350003.
Hegseth, E.N., Tverberg, V., 2013. Effect of Atlantic water inflow on timing of the phytoplankton spring bloom in a high Arctic fjord (Kongsfjorden, Svalbard). J. Mar. Syst. 113–114, 94–105. https://doi.org/10.1016/j.jmarsys.2013.01.003.
Holding, J.M., Duarte, C.M., Delgado-Huertas, A., Soetaert, K., Vonk, J.E., Agustí, S., Wassmann, P., Middelburg, J.J., 2017. Autochthonous and allochthonous contributions of organic carbon to microbial food webs in Svalbard fjords. Limnol. Oceanogr. 62, 1307–1323. https://doi.org/10.1002/lno.10526.
Howes, E.L., Joos, F., Eakin, C.M., Gattuso, J.-P., 2015. An updated synthesis of the observed and projected impacts of climate change on the chemical, physical and biological processes in the oceans. Front. Mar. Sci. 2, 36. https://doi.org/10.3389/fmars.2015.00036.
Huber, S.A., Balz, A., Abert, M., Pronk, W., 2011. Characterisation of aquatic humic and non-humic matter with size-exclusion chromatography e organic carbon detection e organic nitrogen detection (LC-OCD-OND). Water Res. 45, 879–885. https://doi.org/10.1016/j.watres.2010.09.023.
IPCC, 2014. Climate Change 2013 - The Physical Science Basis. Fifth Assessment Report, Climate Change 2014: Synthesis Report. Contribution of Working Groups I, II and III to the Fifth Assessment Report of the Intergovernmental Panel on Climate Change. https://doi.org/10.1017/CBO9781107415324.
Isaksen, K., Nordli, Førland, E.J., Łupikasza, E., Eastwood, S., Niedźwiedź, T., 2016. Recent warming on spitsbergen-influence of atmospheric circulation and sea ice cover. J. Geophys. Res. 121, 11–913. https://doi.org/10.1002/2016JD025606.
Iversen, K.R., Seuthe, L., 2011. Seasonal microbial processes in a high-latitude fjord (Kongsfjorden, Svalbard): I. Heterotrophic bacteria, picoplankton and nanoflagellates. Polar Biol. 34, 731–749. https://doi.org/10.1007/s00300-010-0929-2.
Jørgensen, L., Stedmon, C.A., Kragh, T., Markager, S., Middelboe, M., Søndergaard, M., 2011. Global trends in the fluorescence characteristics and distribution of marine dissolved organic matter. Mar. Chem. 126, 139–148. https://doi.org/10.1016/j.marchem.2011.05.002.
Korak, J.A., Dotson, A.D., Summers, R.S., Rosario-Ortiz, F.L., 2014. Critical analysis of commonly used fluorescence metrics to characterize dissolved organic matter. Water Res. 49, 327–338. https://doi.org/10.1016/j.watres.2013.11.025.
Kortsch, S., Primicerio, R., Fossheim, M., Dolgov, A.V., Aschan, M., 2015. Climate change alters the structure of arctic marine food webs due to poleward shifts of boreal generalists. Proc. R. Soc. B Biol. Sci. https://doi.org/10.1098/rspb.2015.1546.
Kowalczuk, P., Tilstone, G.H., Zabłocka, M., Röttgers, R., Thomas, R., Zabłocka, M., Röttgers, R., Thomas, R., 2013. Composition of dissolved organic matter along an Atlantic meridional transect from fluorescence spectroscopy and parallel factor analysis. Mar. Chem. 157, 170–184. https://doi.org/10.1016/j.marchem.2013.10.004.
Lapierre, J.F., Del Giorgio, P.A., 2014. Partial coupling and differential regulation of biologically and photochemically labile dissolved organic carbon across boreal aquatic networks. Biogeosciences 11, 5969–5985. https://doi.org/10.5194/bg-11-5969-2014.
Lawaetz, A.J., Stedmon, C.A., 2009. Fluorescence intensity calibration using the Raman scatter peak of water. Appl. Spectrosc. 63, 936–940. https://doi.org/10.1366/000370209788964548.
Liu, S., Lim, M., Fabris, R., Chow, C.W.K., Drikas, M., Korshin, G., Amal, R., 2010. Multi-wavelength spectroscopic and chromatography study on the photocatalytic oxidation of natural organic matter. Water Res. 44, 2525–2532. https://doi.org/10.1016/j.watres.2010.01.036.
Logue, J.B., Stedmon, C.A., Kellerman, A.M., Nielsen, N.J., Andersson, A.F., Laudon, H., Lindström, E.S., Kritzberg, E.S., 2016. Experimental insights into the importance of aquatic bacterial community composition to the degradation of dissolved organic matter. ISME J 10, 533–545. https://doi.org/10.1038/ismej.2015.131.
Luckman, A., Benn, D.I., Cottier, F., Bevan, S., Nilsen, F., Inall, M., 2015. Calving rates at tidewater glaciers vary strongly with ocean temperature. Nat. Commun. 6, 8566. https://doi.org/10.1038/ncomms9566.
Mayer, L.M., Schick, L.L., Loder, T.C., 1999. Dissolved protein fluorescence in two Maine estuaries. Mar. Chem. 64, 171–179. https://doi.org/10.1016/S0304-4203(98)00072-3.
Müller, S., Vähätalo, A.V., Granskog, M.A., Autio, R., Kaartokallio, H., 2011. Behaviour of dissolved organic matter during formation of natural and artificially grown Baltic Sea ice. Ann. Glaciol. 52, 233–241. https://doi.org/10.3189/172756411795931886.
Müller, S., Vähätalo, A.V., Stedmon, C.A., Granskog, M.A., Norman, L., Aslam, S.N., Underwood, G.J.C., Dieckmann, G.S., Thomas, D.N., 2013. Selective incorporation of dissolved organic matter (DOM) during sea ice formation. Mar. Chem. 155, 148–157. https://doi.org/10.1016/j.marchem.2013.06.008.
Murphy, K.R., Stedmon, C.A., Graeber, D., Bro, R., 2013. Fluorescence spectroscopy and multi-way techniques. PARAFAC. Anal. Methods 5, 6557. https://doi.org/10.1039/c3ay41160e.
Murphy, K.R., Stedmon, C.A., Wenig, P., Bro, R., 2014. OpenFluor- an online spectral library of auto-fluorescence by organic compounds in the environment. Anal. Methods 6, 658–661. https://doi.org/10.1039/C3AY41935E.
Nimptsch, J., Woelfl, S., Osorio, S., Valenzuela, J., Ebersbach, P., von Tuempling, W., Palma, R., Encina, F., Figueroa, D., Kamjunke, N., Graeber, D., 2015. Tracing dissolved organic matter (DOM) from land-based aquaculture systems in North Patagonian streams. Sci. Total Environ. 537, 129–138. https://doi.org/10.1016/J.SCITOTENV.2015.07.160.
Norman, L., Thomas, D.N., Stedmon, C.a., Granskog, M.a., Papadimitriou, S., Krapp, R.H., Meiners, K.M., Lannuzel, D., van der Merwe, P., Dieckmann, G.S., 2011. The characteristics of dissolved organic matter (DOM) and chromophoric dissolved organic matter (CDOM) in Antarctic sea ice. Deep Sea Res. Part II Top. Stud. Oceanogr. 58, 1075–1091. https://doi.org/10.1016/j.dsr2.2010.10.030.
Noufal, K.K., Najeem, S., Latha, G., Venkatesan, R., 2017. Seasonal and long term evolution of oceanographic conditions based on year-around observation in Kongsfjorden, Arctic Ocean. Polar Sci. 11, 1–10. https://doi.org/10.1016/j.polar.2016.11.001.
Oren, A., Gunde-Cimerman, N., 2007. Mycosporines and mycosporine-like amino acids: UV protectants or multipurpose secondary metabolites? FEMS Microbiol. Lett. 269, 1–10. https://doi.org/10.1111/j.1574-6968.2007.00650.x.
Osburn, C.L., Retamal, L., Vincent, W.F., 2009. Photoreactivity of chromophoric dissolved organic matter transported by the Mackenzie River to the Beaufort Sea. Mar. Chem. 115, 10–20. https://doi.org/10.1016/j.marchem.2009.05.003.
Osterholz, H., Dittmar, T., Niggemann, J., 2014. Molecular evidence for rapid dissolved organic matter turnover in Arctic fjords. Mar. Chem. 160, 1–10. https://doi.org/10.1016/j.marchem.2014.01.002.
Osterholz, H., Singer, G., Wemheuer, B., Daniel, R., Simon, M., Niggemann, J., Dittmar, T., 2016. Deciphering associations between dissolved organic molecules and bacterial communities in a pelagic marine system. ISME J 10, 1717. https://doi.org/10.1038/ismej.2015.231.
Overland, J.E., Wang, M., 2013. When will the summer Arctic be nearly sea ice free? Geophys. Res. Lett. 40, 2097–2101. https://doi.org/10.1002/grl.50316.
Parson, T.R., Maita, Y., Lalli, C.M., 1984. A manual of chemical and biological methods for seawater analysis. A Manual of Chemical and Biological Methods for Seawater Analysis https://doi.org/10.1016/B978-0-08-030287-4.50002-5.
Pavlov, A.K., Silyakova, A., Granskog, M.A., Bellerby, R.G.J., Engel, A., Schulz, K.G., Brussaard, C.P.D., 2014. Marine CDOM accumulation during a coastal Arctic mesocosm

experiment: no response to elevated pCO2 levels. J. Geophys. Res. Biogeosci. 119, 1216–1230. https://doi.org/10.1002/2013JG002587.
Penru, Y., Simon, F.S.X., Guastalli, A.R., Esplugas, S.S., Llorens, J.J., Baig, S., 2013. Characterization of natural organic matter from Mediterranean coastal seawater. J. Water Supply Res. Technol. - AQUA 62, 42–51. https://doi.org/10.2166/aqua.2013.113.
Poloczanska, E.S., Burrows, M.T., Brown, C.J., García Molinos, J., Halpern, B.S., Hoegh-Guldberg, O., Kappel, C.V., Moore, P.J., Richardson, A.J., Schoeman, D.S., Sydeman, W.J., 2016. Responses of marine organisms to climate change across oceans. Front. Mar. Sci. 3, 62. https://doi.org/10.3389/fmars.2016.00062.
Retelletti Brogi, S., Ha, S.-Y., Kim, K., Derrien, M., Lee, Y.K., Hur, J., 2018. Optical and molecular characterization of dissolved organic matter (DOM) in the Arctic ice core and the underlying seawater (Cambridge Bay, Canada): implication for increased autochthonous DOM during ice melting. Sci. Total Environ. 627, 802–811.
Řezanka, T., Temina, M., Tolstikov, A.G., Dembitsky, V.M., 2004. Natural microbial UV radiation filters — Mycosporine-like amino acids. Folia Microbiol. (Praha). 49, 339–352. https://doi.org/10.1007/BF03354663.
Rosenblatt, A.E., Schmitz, O.J., 2016. Climate change, nutrition, and bottom-up and top-down food web processes. Trends Ecol. Evol. 31, 965–975. https://doi.org/10.1016/j.tree.2016.09.009.
Saba, V.S., Griffies, S.M., Anderson, W.G., Winton, M., Alexander, M.A., Delworth, T.L., Hare, J.A., Harrison, M.J., Rosati, A., Vecchi, G.A., Zhang, R., 2016. Enhanced warming of the Northwest Atlantic Ocean under climate change. J. Geophys. Res. Ocean. 121, 118–132. https://doi.org/10.1002/2015JC011346.
Søndergaard, M., Stedmon, C.a., Borch, N.H., 2003. Fate of terrigenous dissolved organic matter (DOM) in estuaries: aggregation and bioavailability. Ophelia 57, 161–176. https://doi.org/10.1080/00785236.2003.10409512.
Stedmon, C.A., Amon, R.M.W., Rinehart, A.J., Walker, S.A., 2011a. The supply and characteristics of colored dissolved organic matter (CDOM) in the Arctic Ocean: Pan Arctic trends and differences. Mar. Chem. 124, 108–118. https://doi.org/10.1016/j.marchem.2010.12.007.
Stedmon, Colin A., Thomas, D.N., Papadimitriou, S., Granskog, M.A., Dieckmann, G.S., 2011b. Using fluorescence to characterize dissolved organic matter in Antarctic sea ice brines. J. Geophys. Res. Biogeosci. 116, 1–9. https://doi.org/10.1029/2011JG001716.
Svendsen, H., Beszczynska-Møller, A., Hagen, J.O., Lefauconnier, B., Tverberg, V., Gerland, S., Ørbøk, J.B., Bischof, K., Papucci, C., Zajaczkowski, M., Azzolini, R., Bruland, O., Wiencke, C., Winther, J.G., Dallmann, W., 2002. The physical environment of Kongsfjorden-Krossfjorden, and Arctic fjord system in Svalbard. Polar Res. 21, 133–166. https://doi.org/10.1111/j.1751-8369.2002.tb00072.x.
Tverberg, V., Skogseth, R., Cottier, F., Sundfjord, A., Walczowski, W., Inall, M., Falck, E., Pavlova, O., Nilsen, F., 2019. The Kongsfjorden Transect: seasonal and inter-annual variability in hydrography. The Ecosystem of Kongsfjorden, Svalbard, pp. 49–104.
Underwood, G.J.C., Michel, C., Meisterhans, G., Niemi, A., Belzile, C., Witt, M., Dumbrell, A.J., Koch, B.P., 2019. Organic matter from Arctic sea-ice loss alters bacterial community structure and function. Nat. Clim. Chang. 9, 170. https://doi.org/10.1038/s41558-018-0391-7.
Uusikivi, J., Vähätalo, A.V., Granskog, M.A., Sommaruga, R., 2010. Contribution of mycosporine-like amino acids and colored dissolved and particulate matter to sea ice optical properties and ultraviolet attenuation. Limnol. Oceanogr. 55, 703–713. https://doi.org/10.4319/lo.2009.55.2.0703.
Vernet, M., Whitehead, K., 1996. Release of ultraviolet-absorbing compounds by the red-tide dinoflagellate Lingulodinium polyedra. Mar. Biol. 127, 35–44. https://doi.org/10.1007/BF00993641.
Weishaar, J., Aiken, G., Bergamaschi, B., Fram, M., Fujii, R., Mopper, K., 2003. Evaluation of specific ultra-violet absorbance as an indicator of the chemical content of dissolved organic carbon. Environ. Sci. Technol. 37, 4702–4708. https://doi.org/10.1021/es030360x.
Woods, G.C., Simpson, M.J., Pautler, B.G., Lamoureux, S.F., Lafrenière, M.J., Simpson, A.J., 2011. Evidence for the enhanced lability of dissolved organic matter following permafrost slope disturbance in the Canadian High Arctic. Geochim. Cosmochim. Acta 75, 7226–7241. https://doi.org/10.1016/J.GCA.2011.08.013.
Wozniak, B., Dera, J., 2007. Light Absorption in Sea Water, Light Absorption in Sea Water. Springer New York, New York, NY https://doi.org/10.1007/978-0-387-49560-6.
Wünsch, U.J., Acar, E., Koch, B.P., Murphy, K.R., Schmitt-Kopplin, P., Stedmon, C.A., 2018a. The molecular fingerprint of fluorescent natural organic matter offers insight into biogeochemical sources and diagenetic state. Anal. Chem. 90, 14188–14197. https://doi.org/10.1021/acs.analchem.8b02863.
Wünsch, Urban J., Stedmon, C.A., Tranvik, L.J., Guillemette, F., 2018b. Unraveling the size-dependent optical properties of dissolved organic matter. Limnol. Oceanogr. 63, 588–601. https://doi.org/10.1002/lno.10651.
Yang, L., Chen, W., Zhuang, W.-E., Cheng, Q., Li, W., Wang, H., Guo, W., Chen, C.-T.A., Liu, M., 2019. Characterization and bioavailability of rainwater dissolved organic matter at the southeast coast of China using absorption spectroscopy and fluorescence EEM-PARAFAC. Estuar. Coast. Shelf Sci. 217, 45–55. https://doi.org/10.1016/J.ECSS.2018.11.002.